A stochastic strategy integrating wind compensation for trajectory tracking in aircraft motion control*

Luca Deori[1], Simone Garatti[1], Maria Prandini[1]

Abstract— **This paper deals with the problem of steering an aircraft along a reference trajectory while counteracting the wind disturbance. We develop a control strategy where the aircraft nonlinear dynamics, physical limitations on the aircraft maneuverability, and passengers comfort are accounted for by feedback linearization and a suitable convex relaxation of constraints. A probabilistic constraint is introduced to account for the tracking error introduced by the stochastic wind disturbance. Since wind is represented by a Gaussian random field and its characteristics depend on both time and space, we identify on-the-fly a local autoregressive model via recursive least squares with forgetting factor. The probabilistic constraint formulation, the wind model update, and the re-computation of the control action jointly allow to account for the spatial variability of the random field and to obtain recursive feasibility in the receding horizon solution. A randomized method is adopted to obtain a convex relaxation of the resulting chance-constrained optimization problem, which can then be solved on-line, at low computational effort.**

I. INTRODUCTION

In this paper, we address the problem of steering an aircraft along a given reference trajectory by counteracting the action of the wind disturbance, while satisfying constraints related to aircraft physical limitations. To this purpose we develop a stochastic control strategy which rests on the formulation of a chance-constrained optimization problem and on its approximate solution via randomization. The main issues are i) the non linearity of the aircraft dynamics, ii) the stochastic nature of the wind, which is the main source of uncertainty affecting the aircraft motion [3], [15], [9]. We apply feedback linearization so as to obtain a simpler linear model of the aircraft dynamics to embed in the optimization problem formulation. Since the state and input constraints representing aircraft physical limitations become non-convex when expressed in the new coordinates frame, suitable convex relaxations are introduced. The idea of adopting feedback linearization followed by constraint convexification has been studied in [25], [23] and applied to aircraft motion control in [12]. Compared to [12], here, we use a more accurate model of the aircraft dynamics, include the stochastic wind disturbance, and adopt a stochastic approach to address tracking of a reference trajectory. Aircraft motion control is addressed also in [14], [17], [16], where the presence of constraints is only partially accounted for. The issue of counteracting the stochastic wind disturbance compatibly with the other constraints is addressed by introducing suitable probabilistic constraints on the tracking error as suggested in [11], [13], and by adopting a receding horizon implementation of the solution to the resulting chance-constrained optimization problem, leading to a Model Predictive Control (MPC) scheme, [18]. Wind velocity presents a spatial and temporal correlation structure and is described by a Gaussian random field [16], [14], which makes harder to tackle the introduced probabilistic constraints. We then develop a local wind model that provides an accurate description of the wind disturbance in the region around the current aircraft position and that can be adjusted on-line based on the available wind measurements. At each time step, the identified model is used to generate as many sample wind realizations as needed by the scenario theory [5], [7], [8], to provide feasibility guarantees for the randomized solution to the chance-constrained optimization. Eventually, we obtain a convex finite horizon optimization problem which is computationally appealing, whose solution satisfies aircraft motion constraints and is able to track the reference trajectory by counteracting the wind disturbance when applied according to a receding horizon strategy.

II. MODELING FRAMEWORK

A. Aircraft dynamics

The following flat earth, point mass model of the aircraft dynamics is considered:

$$\begin{aligned}
\dot{x} &= V\cos\psi\cos\gamma + w_x & \dot{V} &= -\frac{D}{m} - g\sin\gamma + \frac{T\cos\alpha}{m}\\
\dot{y} &= V\sin\psi\cos\gamma + w_y & \dot{\psi} &= \frac{L+T\sin\alpha}{mV\cos\gamma}\sin\phi\\
\dot{z} &= V\sin\gamma + w_z & \dot{\gamma} &= \frac{L+T\sin\alpha}{mV}\cos\phi - \frac{g}{V}\cos\gamma
\end{aligned}$$

The state variables are the positions x, y, z of the aircraft, the aircraft True Air Speed (TAS) V, the heading angle ψ, the path angle γ. The inputs are the Angle of Attack (AoA) α, the bank angle ϕ and the engine thrust T. The presence of the wind is accounted for by means of the additive stochastic disturbances w_x, w_y, w_z on the aircraft velocity. Eventually, $D = \frac{1}{2}\rho(z)SV^2C_d(1+b_1\alpha+b_2\alpha^2)$ is the drag force that opposes the aircraft motion in the direction of the TAS, $L = \frac{1}{2}\rho(z)SV^2C_l(1+a\alpha)$ is the lift that provides the force to oppose gravity, ρ is the air density, S is the wing surface, m is the aircraft mass which is assumed to be constant, g is gravitational acceleration, and C_d, C_l, b_1, b_2, a are suitable positive aerodynamics coefficients. Though standing on some simplifying assumptions, models like the one here considered are often adopted when addressing air traffic management application [19], [1], [4], [21].

B. Constraints

Following [1], constraints on the state and input variables are enforced in order to account for physical limitations of

*This work is partly supported by the European Commission under project UnCoVerCPS with grant number 643921.

[1]Luca Deori, Simone Garatti, Maria Prandini are with Dipartimento di Elettronica, Informazione e Bioingegneria, Politecnico di Milano, via Ponzio 34/5 20133 Milano, Italy. {luca.deori, simone.garatti, maria.prandini}@polimi.it

the aircraft, comfort of passengers and safety requirements.

$$\begin{array}{ll} \text{Vertical Acceleration } \ddot{z}: & -a_N \le \ddot{z} \le a_N \\ \text{True Air Speed } V: & V_{min} \le V \le V_{max} \\ \text{Longitudinal Acceleration:} & -a_L \le \dot{V} \le a_L \\ \text{Path angle } \gamma: & \gamma_{min} \le \gamma \le \gamma_{max} \\ \text{Bank Angle } \phi: & -\phi_{max} \le \phi \le \phi_{max} \\ \text{Engine Thrust } T: & T_{min} \le T \le T_{max}. \end{array} \quad (1)$$

C. Wind model

The wind velocities w_x, w_y, w_z are modelled as a time varying vector field, obtained as the sum of two contributions: a deterministic term that represents the forecast of the wind, and a stochastic term accounting for the mismatch between forecast and the actual wind faced by the aircraft, that is:

$$w_x = w_{xf} + w_{xs} \quad w_y = w_{yf} + w_{ys} \quad w_z = w_{zf} + w_{zs}.$$

According to [14], [16], the stochastic wind components w_{xs}, w_{ys}, w_{zs} are modelled as a random field where for every x, y, z, t, the wind components $w_{xs}(x,y,z,t)$, $w_{ys}(x,y,z,t)$, $w_{zs}(x,y,z,t)$ are zero mean Gaussian random variables with the following spatio-temporal correlation structure:

$$\begin{aligned} &\mathbb{E}[w_{xs}(x,y,z,t)w_{xs}(x',y',z',t')] = \mathbb{E}[w_{ys}(x,y,z,t)w_{ys}(x',y',z',t')] \\ &\quad = k(z)k(z')e^{-\sigma_1|t-t'|}e^{-\sigma_2\|[x-x' \;\; y-y']\|}e^{-\sigma_3|z-z'|} \\ &\mathbb{E}[w_{zs}(x,y,z,t)w_{zs}(x',y',z',t')] \\ &\quad = k_z(z)k_z(z')e^{-\sigma_{1z}|t-t'|}e^{-\sigma_{2z}\|[x-x' \;\; y-y']\|}e^{-\sigma_{3z}|z-z'|} \\ &\mathbb{E}[w_{xs}(x,y,z,t)w_{ys}(x',y',z',t')] = \mathbb{E}[w_{xs}(x,y,z,t)w_{zs}(x',y',z',t')] \\ &= \mathbb{E}[w_{ys}(x,y,z,t)w_{zs}(x',y',z',t')] = 0 \end{aligned} \quad (2)$$

where $k(z)$ and $k_z(z)$ represent the variance of the wind velocities at a given altitude z and the coefficients σ_1, σ_2, σ_3 and σ_{1z}, σ_{2z}, σ_{3z} regulate the exponential decrease of the correlation between wind velocities at different positions and time instants as their corresponding spatial and temporal distance increases. According to the correlation structure in (2), wind is isotropic with respect to x, y, and wind velocities along different axes are independent. Note that according to this model the wind disturbance has unbounded support. An approach to generate samples of a random field that satisfy the correlation structure in (2) is described in [14], [16].

III. Feedback linearization

In this section, a feedback linearizing control law is computed. Feedback linearization was applied also in [24] but to simpler models of the aircraft. A similar approach to that in [12] is adopted. Here, however, the presence of the angle of attack α in the aircraft dynamics (which is neglected in [12]) and the more accurate description of the aerodynamics forces require an extension of the results in [12], and lead to a more complex feedback linearizing control law. The obtained linear model is then discretized so as to make it readily usable in the MPC framework.
First, we set

$$T = (D + mg\sin\gamma + \tau m)\frac{1}{\cos\alpha}, \quad (3)$$

so obtaining $\dot{V} = \tau$. If we adopt the change of state variables

$$\begin{array}{lll} x_1 = x & x_2 = y & x_3 = z \\ x_4 = V\cos\psi\cos\gamma & x_5 = V\sin\psi\cos\gamma & x_6 = V\sin\gamma \end{array}$$

the equations governing the system evolution become:

$$\dot{x}_1 = x_4 + w_x \quad \dot{x}_2 = x_5 + w_y \quad \dot{x}_3 = x_6 + w_z \quad (4a)$$

$$\dot{x}_4 = \tau\cos\gamma\cos\psi - V\sin\gamma\cos\psi\dot{\gamma} - V\cos\gamma\sin\psi\dot{\psi} = u_1 \quad (4b)$$

$$\dot{x}_5 = \tau\cos\gamma\sin\psi - V\sin\gamma\sin\psi\dot{\gamma} + V\cos\gamma\cos\psi\dot{\psi} = u_2 \quad (4c)$$

$$\dot{x}_6 = \tau\sin\gamma + V\cos\gamma\dot{\gamma} = u_3 \quad (4d)$$

where u_1, u_2, u_3 are the new input of the system. Solving (4b) and (4c) for τ and ϕ gives

$$\tau = \frac{1}{\cos\gamma}(\cos\psi u_1 + \sin\psi u_2 + V\sin\gamma\dot{\gamma}) \quad (5)$$

$$(L + T\sin\alpha)\sin\phi = m(-\sin\psi u_1 + \cos\psi u_2). \quad (6)$$

From (4d) and (5) we obtain:

$$\tau = \cos\gamma(\cos\psi u_1 + \sin\psi u_2 + \tan\gamma u_3). \quad (7)$$

From (4d), (5), (6) the bank angle ϕ can be computed as:

$$\phi = \arctan\left(\frac{v_2\cos\gamma\,\mathrm{sign}(v_1)}{|v_1|}\right), \quad (8)$$

where we set

$$v_1 = u_3 - \tau\sin\gamma + g\cos^2\gamma \quad v_2 = -\sin\psi u_1 + \cos\psi u_2, \quad (9)$$

to ease the notation. As for the angle of attack α, we get:

$$\mathrm{sign}(v_1)m\sqrt{\frac{v_1^2}{\cos^2\gamma} + v_2^2} = L(\alpha) + \tan\alpha(D(\alpha) + mg\sin\gamma + \tau m) \quad (10)$$

For fixed value of v_1, v_2, γ, τ, V, equation (10) can be solved numerically to obtain α. Indeed, it can be shown that, for sensible values of the aerodynamics parameters a, C_l, C_d, b_1, b_2, α is uniquely defined, see [10]. Thus, altogether (3), (7), (8), and the numerical solution of (10) give the nonlinear feedback that makes the dynamics of x_1, x_2, x_3, x_4, x_5, x_6 linear with respect to the new inputs u_1, u_2, u_3 (see (4a)-(4d)). Note that the state (x_1, x_2, x_3), (x_4, x_5, x_6) and input (u_1, u_2, u_3) are the Cartesian components of the aircraft position, the Cartesian components of the aircraft true air velocity and of the accelerations respectively. The original state variables can be recovered from the new ones as follows

$$\begin{array}{lll} x = x_1 & y = x_2 & z = x_3 \\ V = \sqrt{x_4^2 + x_5^2 + x_6^2} & \psi = \arctan\left(\dfrac{x_5}{x_4}\right) & \gamma = \arcsin\left(\dfrac{x_6}{V}\right). \end{array}$$

System (4a)-(4d) is discretized so as to eventually obtain

$$\mathbf{x}_{t+1} = A\mathbf{x}_t + B\mathbf{u}_t + B_w\mathbf{w}_t, \quad (11)$$

where $A = \begin{bmatrix} I_3 & T_sI_3 \\ 0_{3\times3} & I_3 \end{bmatrix}$ $B = \begin{bmatrix} \frac{T_s^2}{2}I_3 \\ T_sI_3 \end{bmatrix}$ $C = \begin{bmatrix} T_sI_3 \\ 0_{3\times3} \end{bmatrix}$, and T_s is the sampling period.

IV. Constraints reformulation

Fix time $t \in \mathbb{N}$ and let us consider the look-ahead time horizon $[t, t+M]$. In this section the constraints introduced in Section II-B are rewritten as constraints on the new state $\mathbf{x}$ and input $\mathbf{u}$ variables over $t+1, \ldots, t+M$ and $t, \ldots, t+M-1$, respectively. For those constraints that were already treated in [12], their convex approximations are just reported without derivations, while as for those constraints that depend on α, the derivation of their convex reformulations is given. Overall the introduced convex constraint reformulations are such that the original constraints are satisfied at least at the first time instant (t for $\mathbf{u}$ and $t+1$ for $\mathbf{x}$), so as to guarantee that they are always satisfied along a receding horizon.

- Vertical Acceleration

$$-a_N \leq u_{3,t+i} \leq a_N \qquad i=0,\dots,M-1. \tag{12}$$

- True Air Speed

$$x_{4,t+i}^2 + x_{5,t+i}^2 + x_{6,t+i}^2 \leq V_{max}^2 \qquad i=1,\dots,M \tag{13}$$
$$\begin{bmatrix}-1 & 0 & 0\end{bmatrix} R_y R_z \begin{bmatrix}x_{4,t+i} & x_{5,t+i} & x_{6,t+i}\end{bmatrix}^T \leq -V_{min}$$

where the rotation matrices $R_z(\psi_t)$, $R_y(\gamma_t)$ are defined as:

$$R_z = \begin{bmatrix}\cos\psi_t & \sin\psi_t & 0\\ -\sin\psi_t & \cos\psi_t & 0\\ 0 & 0 & 1\end{bmatrix} \; R_y = \begin{bmatrix}\cos\gamma_t & 0 & \sin\gamma_t\\ 0 & 1 & 0\\ -\sin\gamma_t & 0 & \cos\gamma_t\end{bmatrix}.$$

- Longitudinal Acceleration

$$\begin{aligned}-a_L \leq &\cos\gamma_t(\cos\psi_t u_{1,t+i} + \sin\psi_t u_{2,t+i} \\ &+ \tan\gamma_t u_{3,t+i}) \leq a_L \qquad i=0,\dots,M-1,\end{aligned} \tag{14}$$

- Path Angle

$$V_{t+i}^{wc^-}\sin\gamma_{min} \leq x_{6,t+i} \leq V_{t+i}^{wc^-}\sin\gamma_{max} \quad i=1,\dots,M, \tag{15}$$

where $V_{t+i}^{wc^-} = \max\{V_t - iT_s a_L, V_{min}\}$, $i=0,\dots,M$.

- Bank Angle

In view of (6), the constraint on the bank angle in (1) can be rewritten as:

$$\begin{aligned}&|-u_{1,t+i}\sin\psi_{t+i} + u_{2,t+i}\cos\psi_{t+i}| \leq \\ &\leq \sin\bar{\phi}\,\frac{L_{t+i} + T_{t+i}\sin\alpha_{t+i}}{m} \qquad i=0,\dots,M-1.\end{aligned} \tag{16}$$

Taking the squares and recalling (10), (9), we get:

$$v_{2,t+i}^2 \tfrac{\cos^2\bar{\phi}}{\sin^2\bar{\phi}}\cos^2\gamma_{t+i} \leq v_{1,t+i}^2 \qquad i=0,\dots,M-1.$$

Due to the limitations on vertical and longitudinal accelerations, and on γ, it can be easily seen than v_1 and $\cos\gamma$ are always positive. Taking the square root we have

$$\begin{aligned}&|-u_{1,t+i}\sin\psi_{t+i} + u_{2,t+i}\cos\psi_{t+i}|\tfrac{\cos\bar{\phi}}{\sin\bar{\phi}}\cos\gamma_{t+i} \leq \\ &\leq u_{3,t+i} + g\cos^2\gamma_{t+i} - \sin\gamma_{t+i}\cos\gamma_{t+i}(u_{1,t+i}\cos\psi_{t+i} + \\ &+ u_{2,t+i}\sin\psi_{t+i} + u_{3,t+i}\tan\gamma_{t+i}) \qquad i=0,\dots,M-1.\end{aligned} \tag{17}$$

Similarly to [12], convexity is recovered replacing ψ_{t+i} and γ_{t+i} in (17) with their initial value γ_t and ψ_t:

$$\begin{aligned}&|-\sin\psi_t u_{1,t+i} + \cos\psi_t u_{2,t+i}|\tfrac{\cos\bar{\phi}}{\sin\bar{\phi}}\cos\gamma_t \leq \\ &\leq u_{3,t+i} + g\cos^2\gamma_t - \sin\gamma_t\cos\gamma_t(u_{1,t+i}\cos\psi_t + \\ &+ u_{2,t+i}\sin\psi_t + \tan\gamma_t u_{3,t+i}) \qquad i=0,\dots,M-1.\end{aligned} \tag{18}$$

Note that, for each i constraint (18) is linear, and for $i=0$ it is exactly equivalent to the original constraint.

- Engine Thrust

Recalling (3), (7), and $\sin\gamma = \frac{x_6}{V}$, the constraint on the engine thrust can be written as:

$$\begin{aligned}T_{min} \leq &\Big(m\cos\gamma_{t+i}(u_{1,t+i}\cos\psi_{t+i} + u_{2,t+i}\sin\psi_{t+i} + \\ &+ u_{3,t+i}\tan\gamma_{t+i}) + D(x_{3,t+i}, V_{t+i}, \alpha_{t+i}) + \\ &+ mg\tfrac{x_{6,t+i}}{V_{t+i}}\Big)\tfrac{1}{\cos\alpha_{t+i}} \leq T_{max} \qquad i=0\dots M-1.\end{aligned} \tag{19}$$

As for V_{t+i}, ψ_{t+i}, γ_{t+i}, $x_{3,t+i}$, following [12], we can replace them with their initial value V_t, ψ_t, γ_t, $x_{3,t}$. The resulting constraint is still non-convex because of its dependence on the angle of attack α_{t+i} which is a control input and cannot be set equal to α_t. We then enforce the constraint robustly with respect to all the possible values that α can take as $u_{1,t}$, $u_{2,t}$, $u_{3,t}$ vary while satisfying the other constraints. More precisely, we first compute the admissible range of values for α, $[\alpha_{min}(\mathbf{x}_t),\ \alpha_{max}(\mathbf{x}_t)]$, where $\alpha_{min}(\mathbf{x}_t)$ and $\alpha_{max}(\mathbf{x}_t)$ are the minimum and the maximum value for α achieved by solving equation (10) when the state is kept fixed to the current value $\mathbf{x}_t$ and the inputs $u_{1,t}$, $u_{2,t}$, $u_{3,t}$ take all the feasible values in accordance to the constraints (12), (14), (15), and (18). We can then enforce on the engine thrust the robust constraint with respect to the values that can be possibly taken by α:

$$\begin{aligned}\tilde{T}_{min} \leq &mg\tfrac{x_{6,t+i}}{V_t} + m\cos\gamma_t(u_{1,t+i}\cos\psi_t + u_{2,t+i}\sin\psi_t + \\ &+ u_{3,t+i}\tan\gamma_t) \leq \tilde{T}_{max} \qquad i=0,\dots,M-1,\end{aligned} \tag{20}$$

where we set

$$\tilde{T}_{min} = \max_{\alpha\in[\alpha_{min}(\mathbf{x}_t),\ \alpha_{max}(\mathbf{x}_t)]}\{T_{min}\cos\alpha - D(x_{3,t}, V_t, \alpha)\}$$
$$\tilde{T}_{max} = \min_{\alpha\in[\alpha_{min}(\mathbf{x}_t),\ \alpha_{max}(\mathbf{x}_t)]}\{T_{max}\cos\alpha - D(x_{3,t}, V_t, \alpha)\}.$$

Constraints (20) are linear, and the introduced approximations are such that the original constraints (19) are satisfied for $i=0$. Further details can be found in [10].

Note that all the derived convex constraints (12),(13), (14), (15), (18), (20) do not depend on the wind disturbance, which affects only x_1, x_2, and x_3 (see (11)).

V. Control Strategy Design

A. Finite horizon optimization problem

Let $(x_1^R(t), x_2^R(t), x_3^R(t))$, and $(\dot{x}_1^R(t), \dot{x}_2^R(t), \dot{x}_3^R(t))$ denote position and velocity associated to the reference trajectory that the aircraft should track. We assume that the reference trajectory has been suitably designed so as to be compatible with the aircraft motion capabilities, see [10]. The aircraft may deviate from the reference trajectory because of wind. We devise a control strategy to steer the aircraft back and make it track the reference trajectory robustly with respect to the wind disturbance. To this purpose, we formulate a finite horizon optimization problem that embeds the linear aircraft dynamics in Section III, the convex aircraft motion constraints in Section IV and additional probabilistic constraints on the tracking error to account for wind. The solution to this optimization problem is then applied over a receding horizon so as to obtain an MPC scheme.

Given the current time t, we define the position error ξ_{t+i} as the difference between the aircraft actual position $x_{1,t+i}$, $x_{2,t+i}$, $x_{3,t+i}$ and the reference position $x_{1,t+i}^R$, $x_{2,t+i}^R$, $x_{3,t+i}^R$, expressed in longitudinal, lateral and vertical components with respect to the reference trajectory:

$$\xi_{t+i} = \begin{bmatrix}\cos(\psi_{R,t+i}) & \sin(\psi_{R,t+i}) & 0\\ -\sin(\psi_{R,t+i}) & \cos(\psi_{R,t+i}) & 0\\ 0 & 0 & 1\end{bmatrix}\left(\begin{bmatrix}x_{1,t+i}\\ x_{2,t+i}\\ x_{3,t+i}\end{bmatrix} - \begin{bmatrix}x_{1,t+i}^R\\ x_{2,t+i}^R\\ x_{3,t+i}^R\end{bmatrix}\right)$$

where $\psi_{R,t+i}$ is the reference heading angle and can be easily computed as $\psi_{R,t+i} = \arctan(\frac{\dot{x}_{R,t+i}}{\dot{y}_{R,t+i}})$. The components of the position error ξ_{t+i} should be ideally kept below some thresholds. However the error ξ depends additively on the wind disturbance $\mathbf{w}$ through x_1, x_2, x_3 (see equation (11)) and $\mathbf{w}$ has unbounded support. Hence, it is not possible to enforce a constraint which holds robustly, for all possible disturbance realizations of $\mathbf{w}$. We, instead, resort to a probabilistic constraint, namely a constraint that has to be satisfied with a given (high) probability $1-\varepsilon$.

$$\mathbb{P}\{|\xi_{t+i}| \leq [h_{L,i}\ h_{l,i}\ h_{v,i}]^T,\ i=1,\ldots,M\} \geq 1-\varepsilon, \quad (21)$$

where ξ_{t+i} is a function of $\mathbf{w}_t,\ldots,\mathbf{w}_{t+i-1}$, and the inequality within the brackets must hold component-wise. Constraint (21) may not be feasible: indeed thresholds $h_{L,i}$, $h_{l,i}$, $h_{v,i}$, $i=1,\ldots,M$ may be not compatible with the disturbance characteristics, the other constraints on the input and on the state, the system initial condition, and the allowed violation ε. Moreover, verifying compatibility a-priori is too difficult and it would strongly depend on the choice of the model for wind disturbance. To address this feasibility issue, we follow the approach of [11], [13], where $h_{L,i}$, $h_{l,i}$, $h_{v,i}$, $i=1,\ldots,M$, are regarded as variables to be minimized, possibly together with other objectives. In our setting, the cost function J of the finite horizon optimization problem is defined as the sum of two terms: one that depends on the input acceleration $\mathbf{u}$ only and accounts for fuel consumption and passenger comfort, and a second term that accounts for the tracking error components $h_{L,i}$, $h_{l,i}$, $h_{v,i}$, $i=1,\ldots,M$:

$$J=\sum_{i=0}^{M-1}\mu_{ud}^{i}\mathbf{u}_{t+i}^{T}R\mathbf{u}_{t+i}+\sum_{i=1}^{M}\mu_{Lc}\mu_{Ld}^{i}h_{L,i}+\mu_{lc}\mu_{ld}^{i}h_{l,i}+\mu_{vc}\mu_{vd}^{i}h_{v,i} \quad (22)$$

where R, μ_{Lc}, μ_{lc}, μ_{vc}, μ_{ud}^i, μ_{Ld}^i, μ_{ld}^i, μ_{vd}^i, $i=1,\ldots,M$, are appropriate weights. Matrix R is chosen as $R = R_{rot}^T R_{nor}^T R_c R_{nor} R_{rot}$, with

$$R_{rot} = \begin{bmatrix} \cos\psi_t & \sin\psi_t & 0 \\ -\sin\psi_t & \cos\psi_t & 0 \\ 0 & 0 & 1 \end{bmatrix}, \quad R_{nor} = \begin{bmatrix} \frac{1}{a_L} & 0 & 0 \\ 0 & \frac{1}{g\tan\bar{\phi}} & 0 \\ 0 & 0 & \frac{1}{a_N} \end{bmatrix}.$$

Note that R_{rot} is a rotation matrix that transforms u_1 and u_2 (namely, the accelerations along the x and y axes) into the longitudinal and lateral accelerations with respect to the initial heading angle ψ_t, whereas R_{nor} is a normalization matrix, chosen according to the limits on the accelerations. Eventually, matrix R_c allows one to weight the longitudinal, lateral and vertical accelerations, which are directly related to fuel consumption and comfort. Matrix R_c together with μ_{Lc}, μ_{lc}, μ_{vc} regulate the relative importance given to input and position error components, so as to achieve a proper trade-off between saving the control input and keeping the position error small, while μ_{ud}^i, μ_{Ld}^i, μ_{ld}^i, μ_{vd}^i, $i=1,\ldots,M$, take value in $(0\ 1]$ and can be used to weight more the first time steps, which are the most important for the actual aircraft behavior because of the adopted receding horizon implementation of the finite horizon control solution.
Finally, given the discrete-time model of Section III, the convex constraints discussed in Section IV, the probabilistic constraint in (21), and the cost function (22), we can formulate the finite horizon optimization problem as follows:

$$\min_{\substack{\mathbf{u}_{t+i}\ i=0\ldots M-1 \\ h_{L,i},h_{l,i},h_{v,i}\ i=1\ldots M}} J \quad (23)$$
$$\text{s.t.} \begin{cases} \text{constraints (12) (13) (14) (15) (18) (20)} \\ \mathbb{P}\{|\xi_{t+i}| \leq [h_{L,i}\ h_{l,i}\ h_{v,i}]^T,\ i=1,\ldots,M\} \geq 1-\varepsilon \end{cases}$$

Note that problem (23) is very hard to solve because of the presence of the probabilistic constraint and of the complex probabilistic model of the wind, which altogether make it non convex. Indeed, $\mathbf{w}$ depends on the aircraft position, which in turn is a function of the input to be optimized. In Section V-B we revisit the wind model so that it can be regarded as a standard additive disturbance, then in Section V-C we use it to solve problem (23) by means of the scenario approach.

B. Modelling wind in the optimization problem

Both the forecast that provides the wind deterministic component, and the random field that models the wind stochastic component introduce a non-linear dependence of the wind velocity on the aircraft position (x_1, x_2, x_3), which compromises the convexity of the optimization problem (23). Indeed, the wind forecast is a look-up table that maps the aircraft position into the wind velocities, and the covariance structure of the wind random field in (2) depends on the position of the aircraft as well. Note however that when the look-ahead horizon is short, optimization at each time step requires the model of the wind in a neighborhood of the current aircraft position only. Since both the deterministic and stochastic components typically show a weak variability in space, the idea is then to build an approximated local model of the wind that does not depend on x_1, x_2 and x_3. This model is updated at each time step so as to track the aircraft change of position in accordance to the receding horizon implementation of the control strategy.
As for the wind deterministic component $\mathbf{w}_{f,t+i}(x_{1,t+i}, x_{2,t+i}, x_{3,t+i})$, $i=0,\ldots,M$, we approximate it with $\hat{\mathbf{w}}_{f,t+i}$ defined, i by i, as the average of the forecast wind over an hyper-rectangle placed around the current aircraft position and oriented so as to cover the region of space that the aircraft should fly into in the finite horizon M according to the current values of TAS, heading and path angles. This way $\hat{\mathbf{w}}_{f,t+i}$ is a function of time only and it is then straightforward to account for it in the optimization problem. Despite its simplicity, this approach works effectively given the limited variability of the wind forecast over the distances traveled in the considered finite prediction horizon.
As for the stochastic components of the wind, we model $\mathbf{w}_{s,t+i}(x_{1,t+i}, x_{2,t+i}, x_{3,t+i})$ over the finite horizon $[t, t+M]$ by means of discrete time stochastic Auto-Regressive (AR) processes, whose parameters at time t are identified based on the past wind values experienced along the aircraft trajectory up to time instant $t-1$. Based on (11), wind velocities along the aircraft trajectory are easily recovered as follows:

$$\begin{bmatrix} w_{x,l} \\ w_{y,l} \\ w_{z,l} \end{bmatrix} = \frac{1}{T_s}\left(\begin{bmatrix} x_{1,l+1} \\ x_{2,l+1} \\ x_{3,l+1} \end{bmatrix} - \begin{bmatrix} x_{1,l} \\ x_{2,l} \\ x_{3,l} \end{bmatrix} - T_s \begin{bmatrix} x_{4,l} \\ x_{5,l} \\ x_{6,l} \end{bmatrix} - \frac{T_s^2}{2}\begin{bmatrix} u_{1,l} \\ u_{2,l} \\ u_{3,l} \end{bmatrix}\right) \quad (24)$$

from which past stochastic wind components $w_{xs,l}$, $w_{ys,l}$, $w_{zs,l}$, $l = 0,1,\dots,t-1$, can be recovered by subtracting the deterministic ones. In turn, these values can be used to recursively identify the following AR models, one for each wind stochastic component:

$$\hat{w}_{xs,l} = \varphi_{xs,l}^T \theta_x + e_{xs,l} \qquad \hat{w}_{ys,l} = \varphi_{ys,l}^T \theta_y + e_{ys,l} \qquad (25)$$
$$\hat{w}_{zs,l} = \varphi_{zs,l}^T \theta_z + e_{zs,l}$$

where $e_{xs} \sim WGN(0,\lambda_x^2)$, $e_{ys} \sim WGN(0,\lambda_y^2)$, $e_{zs} \sim WGN(0,\lambda_z^2)$ (WGN stands for White Gaussian Noise), $\varphi_{js,l} = [\hat{w}_{js,l-1},\dots,\hat{w}_{js,l-k},1]^T$, $j = x,y,z$, are the regressors, k the model order, and θ_x, θ_y, θ_z the model parameter vectors. Note that a 1 is introduced as last element in the regressors so as to account for non zero mean processes, which may arise due to the strong correlation of the wind both in time and space. When a new wind data becomes available via (24), the AR models are updated by using the Recursive Least Square (RLS) algorithm with forgetting factor μ:

$$\begin{cases} \theta_{j,t} = \theta_{j,t-1} + S_{j,t}\varphi_{js,t-1}(w_{js,t-1} - \varphi_{js,t-1}^T \theta_{j,t-1}) \\ S_{j,t} = \frac{1}{\mu}\left(S_{j,t-1} - \frac{S_{j,t-1}\varphi_{js,t-1}\varphi_{js,t-1}^T S_{i,t-1}}{\mu + \varphi_{js,t-1}^T S_{j,t}\varphi_{js,t-1}}\right) \end{cases}$$

$j = x,y,z$. The white noise variances are also estimated as:

$$\lambda_j^2 = \frac{\sum_{i=1}^{t-1} \mu^{t-i}(w_{js,i} - \varphi_{js,i}^T \theta_{j,t})^2}{\sum_{i=1}^{t-1} \mu^{t-i}}, \; j = x,y,z.$$

Note that the dependence of the wind on the position in space is neglected in the AR models. However, since the identification is repeated at each time step and a forgetting factor is introduced so as to discard past data that are no more representative of the current situation, the model is tuned to the wind characteristics in the region of space close to the current aircraft position. Note also that the proposed approach is not making any use of the stochastic wind field model in (2), and it can account for further disturbances than the wind such as model errors, noisy measurements or noisy reconstructions of the state variables, etc. Its usage eventually enforces additional robustness to control design.

The finite horizon optimization problem (23) can be reformulated as follows by simply replacing $\mathbf{w}$ with $\hat{\mathbf{w}} = \hat{\mathbf{w}}_f + \hat{\mathbf{w}}_s$ as given by the proposed approximate wind model:

$$\min_{\substack{\mathbf{u}_{t+i}\; i=0\dots M-1 \\ h_{L,i},\; h_{l,i},\; h_{v,i}\; i=1\dots M}} J \qquad (26)$$
$$\text{s.t.} \begin{cases} \text{constraints (12) (13) (14) (15) (18) (20)} \\ \mathbb{P}\{|\hat{\xi}_{t+i}| \leq [h_{L,i}\; h_{l,i}\; h_{v,i}]^T,\; i = 1,\dots,M\} \geq 1-\varepsilon \end{cases}$$

where $\hat{\xi}_{t+i}$ is the tracking error when $\hat{\mathbf{w}}$ is used in place of $\mathbf{w}$ in the aircraft dynamics (11).

C. Randomized solution to the optimization problem

In order to enhance to computational tractability of problem (26), we resort to the scenario approach, a randomized method to approximately solve chance-constrained problems that was introduced in [5], [7] and applied to stochastic constrained control in [11], [6], [22]. This entails that at each time t, N realizations of the wind disturbance $[\hat{\mathbf{w}}_t^{(j)}\; \hat{\mathbf{w}}_{t+1}^{(j)}\; \dots \hat{\mathbf{w}}_{t+M-1}^{(j)}]^T$, $j = 1,\dots,N$, are generated according to the latest identified wind model (25), initialized with the wind observations $\mathbf{w}_{t-1},\dots,\mathbf{w}_{t-k}$. Then, the probabilistic constraint in (26) is replaced with the N constraints obtained in correspondence of the extracted disturbance realizations:

$$\min_{\substack{\mathbf{u}_{t+i}\; i=0\dots M-1 \\ h_{L,i},\; h_{l,i},\; h_{v,i}\; i=1\dots M}} J \qquad (27)$$
$$\text{s.t.} \begin{cases} \text{constraints (12) (13) (14) (15) (18) (20)} \\ |\xi_{t+i}^{(j)}| \leq [h_{L,i}\; h_{l,i}\; h_{v,i}]^T,\; i = 1\dots M,\; j = 1\dots N \end{cases}$$

where $\xi_{t+i}^{(j)}$ is the tracking error when the aircraft dynamic (11) is evaluated replacing $\mathbf{w}$ with the extracted realization $\hat{\mathbf{w}}^{(j)}$. Note that the new N constraints replacing the probabilistic one are linear constraints, and, overall, (27) is a quadratically constrained quadratic program which can be very efficiently solved by means of standard solvers. Moreover, despite its apparent naivety, the scenario approach is grounded on a solid theory that links N to a precise guarantee on the feasibility of the solution obtained solving problem (27) for the original chance-constrained problem (26), [7], [8], [2]. Here, we rely on the results of [22], which account for the fact that the solution is recomputed at each time step over a receding horizon and specialize the scenario theory to the evaluation of the behavior of the obtained closed-loop control. Specifically, let $(\mathbf{u}_t^\star, h_{L,t+1}^\star, h_{l,t+1}^\star, h_{v,t+1}^\star)$ be that part of the solution to problem (27) that refers to the first time instant and let $\mathbf{x}_{t+1}^\star$ and $\xi_{t+1}^\star$ be the corresponding closed-loop aircraft state and position error respectively. Defining $v_t = \begin{cases} 1 & \text{if } \xi_t^\star \leq [h_{L,t}^\star, h_{l,t}^\star, h_{v,t}^\star]^T \\ 0 & \text{otherwise} \end{cases}$, it then holds that $\lim_{t\to\infty}\inf \frac{1}{t}\sum_{j=0}^{t} v_j \geq 1 - \frac{\zeta}{N+1}$, where ζ is the so called support rank, [22], of the constraints corresponding to the first time instant only (in our setup $\zeta = 6$). In words, the above results means that the receding horizon violation of the constraint, i.e. the proportion of times in which the actual position error $\xi_t^\star$ is within the bounds $h_{L,t}^\star$, $h_{l,t}^\star$, $h_{v,t}^\star$, is kept under control by wisely selecting N. In particular, to guarantee that the receding horizon violation of the constraint is $\geq 1-\varepsilon$, it is enough to choose $N \geq \frac{\zeta}{\varepsilon} - 1$.

VI. NUMERICAL RESULTS

We suppose that the aircraft initial state is $\mathbf{x}_0 = [-60\;\; -6\;\; 6\;\; 600\;\; 600\;\; 0]^T$ (positions are in km, velocities in km/h), which is also the beginning of the reference trajectory, and we use the adopted control strategy for 900 steps with a sampling time $T_s = 2$s. We set the prediction horizon $M = 20$, and the weights: $\mu_{Lc} = 8$, $\mu_{lc} = 6$, $\mu_{vc} = 6$, $\mu_{Ld} = \mu_{ld} = \mu_{vd} = \mu_{ud} = 0.72$, $R_c = diag(0.125,\, 1,\, 0.25)$. The desired ε is set to 0.1, the corresponding number of sample wind realizations is $N = 59$. The bounds for the constraints on aircraft physical limitations are set as: $V_{max} = 910$km/h, $V_{min} = 600$km/h, $\gamma_{max} = 5^\circ$, $\gamma_{min} = -3^\circ$, $T_{max} = 2 \cdot 276$kN, $T_{min} = T_{max}/200$, $a_N = 1.5$m/s^2, $a_L = 0.6$m/s^2, $\bar{\phi} = 40^\circ$. The stochastic wind random field parameters are set as: $\sigma_1 = \sigma_{1z} = 6\,10^{-4}$, $\sigma_2 = 1.6\,10^{-5}$, $\sigma_3 = 1.5\,10^{-4}$, $\sigma_{2z} = 1.5\,10^{-4}$, $\sigma_{3z} = 1.6\,10^{-5}$, $k(z) = \frac{z}{3} + 5$, $k_z(z) = 0.5(\frac{z}{3} + 5)$.

In the simulation the wind faced by the aircraft is generated according to the wind model in Section II-C. As for the wind forecast w_{xf}, w_{yf}, w_{zf}, we rely on the NOAA Rapid Refresh (RAP) model [20]. The controller recovers the past wind values from the knowledge of the state according to

(24). The so obtained wind data are exploited to recursively identify three AR models of order $k = 3$, as described in Section V-B, which are used to generate the wind sample realizations as required for the application of the scenario approach.

The results achieved by implementing the proposed approach are reported in Figure 1, where a 3-D view of the actual trajectory of the aircraft, along with the reference trajectory, is depicted. The reference trajectory is well followed by the aircraft and the position error keeps almost always below 100m (see Figure 2) and it is usually even smaller especially on the lateral and vertical components. The computed $h^{\star}_{L,t}$, $h^{\star}_{l,t}$, $h^{\star}_{v,t}$ provides a good bound on the actual position error: the first step position constraint is violated, namely $|\xi_t|$ is greater than the corresponding bound $[h^{\star}_{L,t}\ h^{\star}_{l,t}\ h^{\star}_{v,t}]$ computed at time $t-1$, only in the 5.2% of the steps.

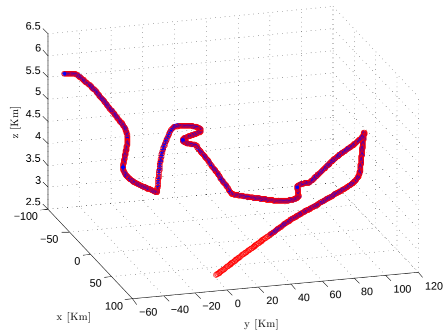

Fig. 1: Aircraft trajectory: receding horizon solution (blue stars), reference trajectory (red circle).

Considering the same set-up, we perform a simulation where the same wind realization acts on the aircraft, but the wind is not accounted for in the control design, namely we set $\hat{\mathbf{w}} = 0$ in the finite horizon optimization problem. The comparison between the position error ξ obtained accounting for the wind presence or neglecting it in the optimization problem is reported in Figure 2. The position error obtained without accounting for the wind is greater than the one obtained accounting for the wind presence in the optimization problem, indeed we get that neglecting the wind $\sum_{t=1}^{900} |\xi_t|$ results [60.47 27.40 7.80], while accounting for the wind we achieve a much better performance [8.74 2.98 0.93].

Fig. 2: Absolute value of the position error ξ obtained when accounting for the wind presence (red) and when neglecting the presence of the wind (green).

References

[1] Eurocontrol experimental center. user manual for the base of aircraft data (BADA) revision 3.10, 2010.

[2] T. Alamo, R. Tempo, A. Luque, and D.R. Ramirez. Randomized methods for design of uncertain systems: Sample complexity and sequential algorithms. *Automatica*, 52:160–172, 2015.

[3] S.G. Benjamin, B.E. Schwartz, E.J. Szoke, and S.E. Koch. The value of wind profiler data in us weather forecasting. *Bulletin of the American Meteorological Society*, 85(12), 2004.

[4] K. P. Bollino. *High-Fidelity Real-Time Trajectory Optimization for Reusable Launch Vehicles*. PhD thesis, Naval Postgraduate School, Monterey, California, 2006.

[5] G. Calafiore and M.C. Campi. The scenario approach to robust control design. *IEEE Transactions on Automatic Control*, 51(5), 2006.

[6] G.C. Calafiore and L. Fagiano. Robust model predictive control via scenario optimization. *Automatic Control, IEEE Transactions on*, 58(1):219–224, 2013.

[7] M.C. Campi and S. Garatti. The exact feasibility of randomized solutions of uncertain convex programs. *SIAM Journal on Optimization*, 19(3):1211–1230, 2008.

[8] M.C. Campi, S. Garatti, and M. Prandini. The scenario approach for systems and control design. *Annual Reviews in Control*, 33(2), 2009.

[9] G. Chaloulos and J. Lygeros. Effect of Wind Correlation on Aircraft Conflict Probability. *AIAA Journal of Guidance, Control, and Dynamics*, 30(6):1742–1752, 2007.

[10] L. Deori. *A Model Predictive Control approach to aircraft motion control*. PhD thesis, Politecnico di Milano, Milan, Italy, 2015.

[11] L. Deori, S. Garatti, and M. Prandini. Stochastic constrained control: trading performance for state constraint feasibility. In *Proceedings of the 2013 European Control Conference*, 2013.

[12] L. Deori, S. Garatti, and M. Prandini. A model predictive control approach to aircraft motion control. In *American Control Conference (ACC), 2015*, pages 2299–2304, 2015.

[13] L. Deori, S. Garatti, and M. Prandini. Stochastic control with input and state constraints: A relaxation technique to ensure feasibility. In *54th IEEE Conference on Decision and Control*, 2015.

[14] W. Glover and J. Lygeros. A stochastic hybrid model for air traffic control simulation. In *Hybrid Systems: Computation and Control*, pages 372–386. Springer, 2004.

[15] J. Hu, M. Prandini, and S. Sastry. Aircraft conflict prediction in presence of a spatially correlated wind field. *IEEE Transactions on Intelligent Transportation Systems*, 6(3):326–340, 2005.

[16] I. Lymperopoulos. *Sequential Monte Carlo methods in air traffic management*. PhD thesis, Diss., Eidgenössische Technische Hochschule ETH Zürich, Nr. 19004, 2010.

[17] I. Lymperopoulos, J. Lygeros, A. Lecchini Visintini, J. M. Maciejowski, and W. Glover. A Stochastic Hybrid Model for Air Traffic Management Processes. Technical report, Cambridge, 2007.

[18] J.M. Maciejowski. *Predictive control: with constraints*. Pearson education, 2002.

[19] K. Margellos and J. Lygeros. Toward 4D Trajectory Management in Air Traffic Control: A Study Based on Monte Carlo Simulation and Reachability Analysis. *IEEE Transactions on Control Systems Technology*, 21(5):1820–1833, September 2013.

[20] NOAA. Rapid refresh. http://rapidrefresh.noaa.gov/.

[21] R.B. Patel and P.J. Goulart. Trajectory generation for aircraft avoidance maneuvers using online optimization. *Journal of guidance, control, and dynamics*, 34(1):218–230, 2011.

[22] G. Schildbach, L. Fagiano, C. Frei, and M. Morari. The scenario approach for stochastic model predictive control with bounds on closed-loop constraint violations. *Automatica*, 50(12):3009–3018, 2014.

[23] D. Simon, J. Löfberg, and T. Glad. Nonlinear model predictive control using feedback linearization and local inner convex constraint approximations. In *Proceedings of the 2013 European Control Conference*, pages 2056–2061, 2013.

[24] D.M. Stipanović, G. Inalhan, R. Teo, and C.J. Tomlin. Decentralized overlapping control of a formation of unmanned aerial vehicles. *Automatica*, 40(8):1285–1296, 2004.

[25] W.R. Van Soest, Q.P. Chu, and J.A. Mulder. Combined feedback linearization and constrained model predictive control for entry flight. *Journal of Guidance, Control, and Dynamics*, 29(2):427–434, 2006.